On the $P\bar{P}$ Single Diffraction Dissociation at High Energies

A.A. Arkhipov
Institute for High Energy Physics
Protvino, 142284 Moscow Region, Russia

Abstract

It is shown that the suggested three-body forces approach to the dynamics of one-particle inclusive reactions allows to describe excellently the data on the $p\bar{p}$ single diffraction dissociation cross-sections at high energies.

1 Introduction

The last experimental measurement of $p\bar{p}$ single diffraction dissociation at c.m.s. energies $\sqrt{s} = 546$ and $1800\ GeV$, carried out by CDF group at the Fermilab Tevatron collider, has shown that the popular model of supercritical Pomeron does not describe the existing experimental data.

The statement, made in paper [1], is as follows: the value of $\sigma_{SD}^{p\bar{p}} = (7.89 \pm 0.33)\ mb$, measured at $\sqrt{s} = 546\ GeV$, is extrapolated by the supercritical Pomeron model to $\sigma_{SD}^{p\bar{p}} = (13.9 \pm 0.9)\ mb$ at $\sqrt{s} = 1800\ GeV$, while the measured value at this energy is equal to $\sigma_{SD}^{p\bar{p}} = (9.45 \pm 0.44)\ mb$. The ratio of the measured $\sigma_{SD}^{p\bar{p}}$ to that obtained by extrapolation is

$$\frac{\sigma_{SD}^{p\bar{p}}(experimental)}{\sigma_{SD}^{p\bar{p}}(extrapolation)}(\sqrt{s} = 1800\ GeV) = 0.68 \pm 0.05. \tag{1}$$

Besides that, at $\sqrt{s} = 20\ GeV$ the experimental $\sigma_{SD}^{p\bar{p}} = (4.9 \pm 0.55)\ mb$ is 4.5 times larger than the value $\sigma_{SD}^{p\bar{p}} = (1.1 \pm 0.17)\ mb$, obtained by the extrapolation of the measured value of $\sigma_{SD}^{p\bar{p}}$ at $\sqrt{s} = 546\ GeV$ down to $\sqrt{s} = 20\ GeV$ with the help of the supercritical Pomeron model.

The emerging situation can be considered as a supercrisis for the supercritical Pomeron model. Obviously, the foundations of this model require further theoretical study and the construction of newer, more general phenomenological framework which would enable to remove the discrepancy between the model predictions and experiment. In relation to this, one should note the paper [2], where an attempt to save the supercritical Pomeron model has been undertaken.

Another approach to the dynamical description of one-particle inclusive reactions has been proposed in [3]. The consideration, presented in this paper, revealed several fundamental properties of one-particle inclusive cross-sections in the region of diffraction dissociation. In particular, it was shown that the slope of the diffraction cone in $p\bar{p}$ single diffraction dissociation is related to the effective radius of three-nucleon forces in the same way as the slope of the diffraction cone in elastic $p\bar{p}$ scattering is related to the effective radius of two-nucleon forces. It was also demonstrated that the effective radii of two- and three-nucleon forces, which are the characteristics of elastic and inelastic interactions of two nucleons, define the structure of the $p\bar{p}$ total cross-sections in a simple and physically transparent form.

In the work [31] a more detailed analysis of the experimental data on $p\bar{p}$ total cross-sections and the slope of the diffraction cone in elastic $p\bar{p}$ scattering has been performed. This allowed us to extract the effective radius of three-nucleon forces. Here I shall show that the suggested approach to the dynamics of one-particle inclusive reactions gives an excellent quantitative description of the experimental data on the $p\bar{p}$ single diffraction dissociation cross-sections at high energies.

First of all let me remind the basic statements of three-body forces approach to the dynamical description of one-particle inclusive reactions.

2 Three-body forces in relativistic quantum theory

Using the LSZ or Bogoljubov reduction formulae in quantum field theory [32], we can easily obtain the following cluster structure for a $3 \to 3$ scattering amplitude (see Fig. 1)

$$\mathcal{F}_{123} = \mathcal{F}_{12} + \mathcal{F}_{23} + \mathcal{F}_{13} + \mathcal{F}^C_{123} \tag{2}$$

where $\mathcal{F}_{ij}, (i, j = 1, 2, 3)$ are $2 \to 2$ scattering amplitudes, $\mathcal{F}^C_{123}$ is called the connected part of the $3 \to 3$ scattering amplitude.

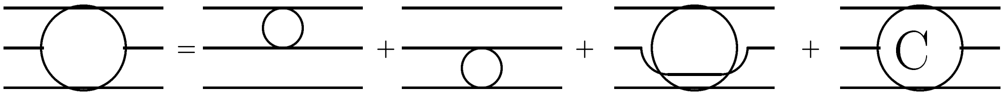

Fig. 1.

In the framework of single-time formalism in quantum field theory [33] we construct the $3 \to 3$ scattering amplitude $T_{123}(E)$ off energy shell with the same (cluster) structure as (2)

$$T_{123}(E) = T_{12}(E) + T_{23}(E) + T_{13}(E) + T^C_{123}(E). \tag{3}$$

The three particle interaction quasipotential $V_{123}(E)$ is related to the off-shell $3 \to 3$ scattering amplitude $T_{123}(E)$ by the Lippmann-Schwinger-type equation

$$T_{123}(E) = V_{123}(E) + V_{123}(E)G_0(E)T_{123}(E). \tag{4}$$

There is the same transformation between two particle interaction quasipotentials V_{ij} and off energy shell $2 \to 2$ scattering amplitudes T_{ij}

$$T_{ij}(E) = V_{ij}(E) + V_{ij}(E)G_0(E)T_{ij}(E). \tag{5}$$

It can be shown that in the quantum field theory the three particle interaction quasipotential has the following structure [35]

$$V_{123}(E) = V_{12}(E) + V_{23}(E) + V_{13}(E) + V_0(E). \tag{6}$$

The quantity $V_0(E)$ is called the quasipotential of three-body forces. $V_0(E)$ represents the defect of three particle interaction quasipotential over the sum of two particle interaction quasipotentials and describes the true three-body interactions.

The scattering amplitude relevant to three-body forces to is related to the quasipotential of the three-body forces by the equation

$$T_0(E) = V_0(E) + V_0(E)G_0(E)T_0(E). \tag{7}$$

It should be stressed that the three-body forces appear as a result of consistent consideration of three-body problem in the framework of local quantum field theory.

3 Global analyticity of the scattering amplitude relevant to three-body forces (SA3BF)

Let us introduce the following useful notations

$$< p'_1 p'_2 p'_3 | S - 1 | p_1 p_2 p_3 >= 2\pi\delta^4 (\sum_{i=1}^{3} p'_i - \sum_{j=1}^{3} p_j) \mathcal{F}_{123}(s; \hat{e}', \hat{e}), \tag{8}$$

$$s = (\sum_{i=1}^{3} p'_i)^2 = (\sum_{j=1}^{3} p_j)^2.$$

$\hat{e}', \hat{e} \in S_5$ are two unit vectors on the five-dimensional sphere describing the configuration of three-body system in initial and final states (before and after scattering).

We will denote the quantity T_0 restricted on the energy shell as

$$T_0 \mid_{on\, energy\, shell} = \mathcal{F}_0.$$

With the account for the introduced notations the unitarity condition for the quantity $\mathcal{F}_0$ can be written in the form [38, 39]

$$\begin{aligned} Im\mathcal{F}_0(s;\hat{e}',\hat{e}) &= \\ &= \pi A_3(s) \int d\Omega_5(\hat{e}'')\mathcal{F}_0(s;\hat{e}',\hat{e}'') \stackrel{*}{\mathcal{F}}_0 (s;\hat{e},\hat{e}'') + H_0(s;\hat{e}',\hat{e}), \end{aligned} \tag{9}$$

$$Im\mathcal{F}_0(s;\hat{e}',\hat{e}) = \frac{1}{2i}\left[\mathcal{F}_0(s;\hat{e}',\hat{e}) - \stackrel{*}{\mathcal{F}}_0 (s;\hat{e},\hat{e}')\right],$$

where

$$A_3(s) = \Gamma_3(s)/S_5,$$

$\Gamma_3(s)$ is the three-body phase-space volume, S_5 is the volume of the unit five-dimensional sphere. H_0 defines the contribution of all inelastic channels emerging due to three-body forces.

Let us introduce a special notation for the scalar product of two unit vectors $\hat{e}'$ and $\hat{e}$

$$\cos\omega = \hat{e}^{'} \cdot \hat{e}. \tag{10}$$

We will use another notation for SA3BF as well

$$\mathcal{F}_0(s;\hat{e}',\hat{e}) = \mathcal{F}_0(s;\eta,\cos\omega),$$

where all other variables are denoted through η.

Now we are able to go to the formulation of our basic assumption about the analyticity properties for SA3BF [38, 39].

We will assume that for physical values of the variable s and fixed values of η the amplitude $\mathcal{F}_0(s;\eta,\cos\omega)$ is an analytical function of the variable $\cos\omega$ in the ellipse $E_0(s)$ with the semi-major axis

$$z_0(s) = 1 + \frac{M_0^2}{2s} \tag{11}$$

and for any $\cos\omega \in E_0(s)$ and physical values of η it is polynomially bounded in the variable s. M_0 is a constant having dimensionality of mass.

Such analyticity of SA3BF was called a global one. The global analyticity may be considered as a direct generalization of the known analytical properties of two-body scattering amplitude rigorously proved in the local quantum field theory.

At the same time the global analyticity gives us the generalized asymptotic bounds. For example the generalized asymptotic bound for the $O(6)$-invariant SA3BF looks like [38, 39]

$$Im\,\mathcal{F}_0(s;...) \leq \text{Const}\, s^{3/2}\left(\frac{\ln s/s_0}{M_0}\right)^5 = \text{Const}\, s^{3/2} R_0^5(s), \tag{12}$$

where $R_0(s)$ is the effective radius of the three-body forces

$$R_0(s) = \frac{\Lambda_0}{\sqrt{s}} = \frac{r_0}{M_0}\ln\frac{s}{s_0}, \tag{13}$$

r_0 is defined by the power of growth of the amplitude $\mathcal{F}_0$ at high energies [39], M_0 defines the semi-major axis of the global analyticity ellipse (11), Λ_0 is effective global orbital momentum.

It is well known that the Froissart asymptotic bound allows for direct experimental verification because with the help of the optical theorem we can connect the imaginary part of $2 \to 2$ scattering amplitude with the experimentally measurable quantity which is the total cross section. So, if we want to have a possibility for the experimental verification of the generalized asymptotic bounds ($n \geq 3$) we have to establish a connection between the scattering amplitudes relevant to many-body forces and the experimentally measurable quantities. For this aim we have considered the problem of high energy particle scattering from deuteron and this way we found the connection of SA3BF with the experimentally measurable quantity which is the total cross section for scattering from deuteron [36].

Moreover, the relation of SA3BF to one-particle inclusive cross sections has been established [37]. This relation will be the subject of the next section.

4 Three-body forces and diffractive dissociation processes

From the analysis of the problem of high-energy particle scattering from deuteron [37] the formula connecting one-particle inclusive cross sections with the imaginary part of SA3BF was derived. This formula looks like

$$2E_N(\vec{\Delta})\frac{d\sigma}{d\vec{\Delta}}(s,\vec{\Delta}) = (2\pi)^3\frac{M_N}{E_N(\vec{\Delta})}\frac{\chi(\bar{s})}{\bar{s}}Im\mathcal{F}_0(\bar{s};-\vec{\Delta},\vec{\Delta},\vec{q};\vec{\Delta},-\vec{\Delta},\vec{q}), \tag{14}$$

where the function $\chi(s)$ describes the (screening) effects due to interaction of initial and final states (see details in [3, 30, 37] and references therein). For this function it was obtained the expression [3]

$$\chi(s) = \frac{\sigma_N(s)}{2\pi[B_N(s)+R_0^2(s)]} - 1, \tag{15}$$

$B_N(s)$ is the slope of the forward diffraction peak in the elastic scattering from nucleon.

From the generalized asymptotic theorem (12) follows the asymptotic behaviour for $\chi(s)$ admitted by unitarity

$$\chi(s) \sim \frac{1}{\sqrt{s}\ln^3 s}, \quad s\to\infty. \tag{16}$$

The configuration of particles momenta and kinematical variables are shown in Fig. 2. The variable $\bar{s}$ in the R.H.S. of Eq. (14) is related to the kinematical variables of the one-particle inclusive reaction by the equation

$$\begin{aligned}\bar{s} &= 2(s+M_N^2) - M_X^2, \\ t &= -4\Delta^2.\end{aligned} \tag{17}$$

The simple model for the three-body forces considered in [3] gives us the following result for the one-particle inclusive cross section in the region of diffraction dissociation

$$\begin{aligned}\frac{s}{\pi}\frac{d\sigma}{dtdM_X^2} &= (2\pi)^3\frac{\chi(\bar{s})f_0(\bar{s})}{\bar{s}}\exp\left[\frac{R_0^2(\bar{s})}{2}t\right] \\ &\simeq C\sqrt{s_0}\frac{(\ln\bar{s}/s_0)^2}{M_0^5}\exp\left[\frac{R_0^2(\bar{s})}{2}t\right], \quad s\to\infty.\end{aligned} \tag{18}$$

If we take the usual parameterization for one-particle inclusive cross section in the region of diffraction dissociation

$$\frac{s}{\pi}\frac{d\sigma}{dtdM_X^2} = A(s.M_X^2)\exp[b(s,M_X^2)t], \tag{19}$$

we obtain for the quantities A and b

$$A(s,M_X^2) = C\sqrt{s_0}\frac{(\ln\bar{s}/s_0)^2}{M_0^5}, \tag{20}$$

$$b(s,M_X^2) = \frac{R_0^2(\bar{s})}{2}. \tag{21}$$

Eq. (21) shows that the effective radius of three-body forces is related to the slope of diffraction cone for inclusive diffraction dissociation processes in the same way as the effective radius of two-body forces is related to the slope of diffraction cone in elastic scattering processes.

If we take into account Eq. (17) then it follows from the Eq.(13) that the slope of diffraction cone for inclusive diffraction dissociation processes at fixed energy decreases with the growth of missing mass. This property agrees qualitatively well with the experimentally observable picture.

Hence physically transparent notion of the effective radius of three-body forces, introduced previously as a pure mathematical object, connected with the global analyticity of SA3BF, brings us to the tangible physical interpretation that helps us to create physically visual picture and representation for inclusive

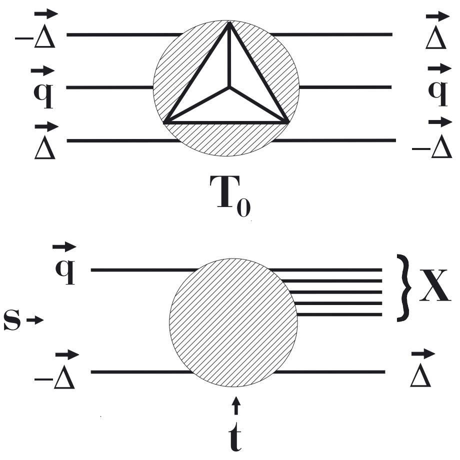

Fig. 2

diffraction dissociation processes at the same level as we can understand and represent elastic scattering processes at high energies.

Besides that, the relation (14) together with linear equation (7) for three-body forces scattering amplitude may be the basis of powerful dynamic apparatus for constructing the dynamical models of theoretical description of the inclusive reactions.

Now we can extract the effective radius of three-nucleon forces from the experimental data on $p\bar{p}$ total cross-sections and the slope of diffraction cone in elastic $p\bar{p}$ scattering.

5 Fit to the data on the $p\bar{p}$ total cross-sections

As a first step, we made a weighted fit to the experimental data on the $p\bar{p}$ total cross-sections, obtained from COMPAS-PPDS database [1]. The values, which were used, are listed in Table I.

The reduced quantities $\sigma_{tot}^{p\bar{p}}/2\pi$ in GeV^{-2} were fitted with the function of the form

$$\sigma_{tot}^{p\bar{p}}/2\pi = a_0 + a_2 \ln^2(\sqrt{s}/\sqrt{s_0}) \tag{22}$$

where a_0, a_2, $\sqrt{s_0}$ are free parameters. We accounted for the experimental errors δx_i by fitting to the experimental points with the weight

$$w_i = \frac{1}{(\delta x_i)^2}. \tag{23}$$

Our fit yielded

$$a_0 = (17.15 \pm 0.06)\ GeV^{-2} \tag{24}$$

[1]The COMPAS database (named Particle Physics Data System - PPDS) can be reached via Internet at http://www.ihep.su, or at its mirror http://muse.lbl.gov:8001/ppds.html

$$a_2 = (0.70 \pm 0.04)\ GeV^{-2} \tag{25}$$
$$\sqrt{s_0} = (18.99 \pm 1.95)\ GeV \tag{26}$$

The result of the fit is shown in Fig. 3.

The quality of the fit can be checked by the extrapolation of the formula (22) to higher energies:

$$\sigma_{tot}^{p\bar{p}}(\sqrt{s} = 16\ TeV) = (119.67 \pm 4.60)\ mb, \tag{27}$$
$$\sigma_{tot}^{p\bar{p}}(\sqrt{s} = 30\ TeV) = (134.85 \pm 5.46)\ mb. \tag{28}$$

These values are consistent with the recent cosmic rays results from Akeno Observatory [4],

$$\sigma_{tot}^{pp}(\sqrt{s} = 30\ TeV) = (120 \pm 15)\ mb. \tag{29}$$

6 Fit to the data on the slope of diffraction cone in elastic $p\bar{p}$ scattering

Compared to the data on the $p\bar{p}$ total cross-sections, the experimental data on the slope of diffraction cone in elastic $p\bar{p}$ scattering are certainly less comprehensive. Therefore, at the first stage we fitted the experimental data on the differential cross-sections in elastic $p\bar{p}$ scattering from Ref. [5]; from this fit we extracted the values of the slope of diffraction cone at five different energies. As a fitting function, we used the linear exponent

$$\frac{d\sigma}{dt} = A\exp(Bt), \tag{30}$$

where A and B were considered as free fit parameters. The obtained fit parameters and the values of χ^2 are listed in Table II.

The obtained five values of the slope, together with the other experimental values from COMPAS database, were used to build a weighted fit of the slope as a function of energy. Table III shows the list of the fitted data. The following parameterization of the slope was assumed:

$$B = b_0 + b_2 \ln^2(\sqrt{s}/\sqrt{s_0}). \tag{31}$$

The value $\sqrt{s_0}$ has been fixed by (26) from the fit to the $p\bar{p}$ total cross-sections. The parameterization (31) is suggested by the asymptotic theorems of the axiomatic quantum field theory. Our fit yielded

$$b_0 = (11.93 \pm 0.15)\ GeV^{-2}, \tag{32}$$
$$b_2 = (0.29 \pm 0.02)\ GeV^{-2}. \tag{33}$$

The fitting curve is shown in Fig. 4.

7 The effective radius of three-nucleon forces and $p\bar{p}$ single diffraction dissociation cross-sections

In paper [3] the asymptotic relation between the slope of diffraction peak in elastic $p\bar{p}$ scattering and the $p\bar{p}$ total cross-section has been obtained. The relation looks like

$$\sigma_{tot}(s) = 2\pi\ [B(s) + R_0^2(s)]. \tag{34}$$

The quantity $R_0^2(s)$ in the R.H.S. of (34) is responsible for the inelastic processes in $p\bar{p}$ interactions. It has a physically transparent notion of the effective radius of three-nucleon forces.

We can use (34) to extract the quantity $R_0^2(s)$ from the experimental data on the $p\bar{p}$ total cross-sections and the slope of diffraction cone in elastic $p\bar{p}$ scattering. Using the fits (22), (31), we obtain

$$R_0^2(s) = [(5.22 \pm 0.21) + (0.41 \pm 0.06)\ln^2(\sqrt{s}/\sqrt{s_0})]\ GeV^{-2}, \qquad \sqrt{s_0} = (18.99 \pm 1.95)\ GeV. \tag{35}$$

The function (35) is plotted in the same Fig. 4, together with the fit to $B(s)$. Fig. 4 also shows the points, denoted by diamonds, for $R_0^2(s)$ obtained earlier [3] .

It is a remarkable fact that the quantity $R_0^2(s)$ defines the slope of the diffraction cone in the $p\bar{p}$ single diffraction dissociation inclusive cross-sections. As it was mentioned above (see details in paper [3]), in the region of diffraction dissociation, one-particle inclusive cross-sections asymptotically can be represented in the form

$$\frac{s}{\pi}\frac{d\sigma}{dtdM_X^2} = A(s.M_X^2)\exp[b(s,M_X^2)t], \tag{36}$$

where

$$A(s,M_X^2) = A\ln^2(\bar{s}/s_0), \tag{37}$$

$$b(s,M_X^2) = \frac{R_0^2(\bar{s})}{2}, \tag{38}$$

$$\bar{s} = 2(s+M_N^2) - M_X^2. \tag{39}$$

Making the corresponding asymptotic estimates, we can easily obtain the following asymptotic formula for the $p\bar{p}$ single diffraction dissociation cross-sections:

$$\sigma_{SD}^{p\bar{p}}(s) = C\frac{\ln^2(s/s_0)}{c_0 + c_2\ln^2(\sqrt{s}/\sqrt{s_0})}, \tag{40}$$

where

$$c_0 = a_0 - b_0, \quad c_2 = a_2 - b_2, \tag{41}$$

the quantities a_0, b_0, a_2, b_2, $\sqrt{s_0}$ are defined by Eqs. (24)-(26), (32), (33) and the constant C is undefined. Let us fix the value of C from the measured $\sigma_{SD}^{p\bar{p}} = (7.89 \pm 0.33)\ mb$ at $\sqrt{s} = 546\ GeV$,

$$C = (1.72 \pm 0.07)\ mb/GeV^2. \tag{42}$$

Then we come to the asymptotic formula for the $p\bar{p}$ single diffraction dissociation cross-sections with all parameters fixed,

$$\sigma_{SD}^{p\bar{p}}(s) = (6.9 \pm 0.3)\frac{\ln^2(\sqrt{s}/\sqrt{s_0})}{(5.22 \pm 0.21) + (0.41 \pm 0.06)\ln^2(\sqrt{s}/\sqrt{s_0})}\ mb, \tag{43}$$
$$\sqrt{s_0} = (18.99 \pm 1.95)\ GeV.$$

From the formula (43) we obtain the value of $\sigma_{SD}^{p\bar{p}}$ at $\sqrt{s} = 1800\ GeV$,

$$\sigma_{SD}^{p\bar{p}} = (10.39 \pm 0.42)\ mb. \tag{44}$$

This value of $\sigma_{SD}^{p\bar{p}}$ is in good agreement with the experimental value $\sigma_{SD}^{p\bar{p}} = (9.46 \pm 0.44)\ mb$ at $\sqrt{s} = 1800\ GeV$ [1].

The extrapolation of the formula (43) up to the LHC energies $\sqrt{s} = 16\ TeV$ gives

$$\sigma_{SD}^{p\bar{p}} = (13.10 \pm 0.53)\ mb. \tag{45}$$

It also follows from the formula (43) that

$$\lim_{s\to\infty}\sigma_{SD}^{p\bar{p}}(s) = (16.78 \pm 0.68)\ mb. \tag{46}$$

We cannot use the equation (43) for the extrapolation down to the lower energies. This formula is an asymptotic one, and one needs to account for the preasymptotic terms when extrapolating to the lower energies. However we can easily take into account the lower energies by introducing the constant preasymptotic term in the numerator of the formula (40). In this case we get

$$\sigma_{SD}^{p\bar{p}}(s) = \frac{A_0 + A_2\ln^2(\sqrt{s}/\sqrt{s_0})}{c_0 + c_2\ln^2(\sqrt{s}/\sqrt{s_0})}, \tag{47}$$

where c_0, c_2 are defined above and A_0, A_2 are to be found from the fit to the experimental data. The experimental values for $p\bar{p}$ single diffraction cross-sections, which were used, are listed in Table IV. Our fit yielded

$$A_0 = 23.395 \pm 2.664, \qquad A_2 = 4.9103 \pm 0.2648. \tag{48}$$

The result of the fit is shown in Fig. 5.

It is remarkable that the fitting curve goes excellently over the experimental points of CDF group at Fermilab.

The experimental data on pp single diffraction dissociation cross sections are plotted in Fig. 6 together with the $p\bar{p}$ data. The rhombes correspond to the data of Armitage et al. [27], triangles to the data of Albrow et al. [28], and circles to the data of Schamberger et al. [29].

We made a new fit taking into account all $p\bar{p}$ data and pp single diffraction cross-sections of Schamberger et al. only. The new fit yielded

$$A_0' = 25.725 \pm 0.265, \qquad A_2' = 4.752 \pm 0.182. \tag{49}$$

Dashed curve in Fig. 6 corresponds to this new fit.

One can see that the results of the fit are mostly determined by the experimental points of the CDF group at Fermilab which have the least statistical errors and among all points show the most regular dependence on the energy of colliding hadrons.

We see also that the account of lower energy data slightly corrects the asymptotic behaviour of single diffraction cross sections at high energies.

8 Conclusion

We have shown that from the generalized asymptotic theorems a la Froissart [34] it follows a simple formula which allows to match the experimental data on $p\bar{p}$ single diffraction dissociation cross sections at high energies including lower energies as well.

Even though the discussed data were published in 1994 and earlier, so far very little progress has been made in its theoretical explanation. At present only the suggested approach allows to describe quantitatively the observed behaviour of $p\bar{p}$ single diffraction dissociation cross sections.

As it has been shown above, the phenomenon of exceedingly moderate energy dependence of single diffraction dissociation cross sections on s observed by CDF at Fermilab is a manifestation of unitarity saturation of three-nucleon forces at Fermilab Tevatron energies. I think that this fact is to be compared with the discovery of the increase of pp total cross sections at CERN ISR and of the growth of K^+p total cross sections revealed at Serpukhov accelerator.

Some time ago many high energy physicists thought that the increase of all hadronic total cross sections was due to the same increase of single diffraction dissociation cross sections. Now we know that this view is wrong and, moreover, we understand why it is not so. In fact, we have found

$$\sigma_{SD}^{p\bar{p}}(s) \longrightarrow \text{Const}, \quad s \to \infty,$$

$$\frac{\sigma_{SD}^{p\bar{p}}(s)}{\sigma_{tot}^{p\bar{p}}(s)} \longrightarrow 0, \quad s \to \infty.$$

I hope that it will be possible to test the obtained results at higher energies, such as those of the LHC collider and even more higher.

Acknowledgements

It is my great pleasure to express thanks to the Organizing Committee, especially to V.I. Savrin and Mrs V. Keshek for their kind invitation and support of my attending this wonderful international meeting held in Samara, to P. Nadolsky for his help in the fitting the experimental data and in preparation of the computer pictures.

References

[1] F. Abe et al., (CDF) Phys. Rev. D 50, 5535 (1994).

[2] E.S. Martynov, B.V. Struminsky, in *Proceedings of the XI-th Workshop on "soft" physics HADRONS-95, Novy Svet, 1995,* eds. G. Bugrij, L. Jenkovsky, E. Martynov (Kiev, 1995), p.53-60.

[3] A.A. Arkhipov, preprint IHEP 96-66, Protvino 1996; in *Proceedings of the XII-th Workshop on "soft" physics HADRONS-96, Novy Svet, 1996,* eds. G. Bugrij, L. Jenkovsky, E. Martynov (Kiev, 1996) p.252-263.

[4] M. Honda et al., Phys. Rev. Lett. 70 525 (1993).

[5] D.D. S. Ayers et al., Phys. Rev. D 15, 3105 (1977).

[6] D. Favart et al., Phys. Rev. Lett. 47, 1191 (1981).

[7] R. L. Cool et al., Phys. Rev. D 24, 2821 (1981).

[8] R. Battiston et al., Phys. Lett. 115B, 333 (1982).

[9] N. Amos et al., Phys. Lett. 120B, 460 (1983).

[10] G. Arnison et al., Phys. Lett. 128B 336 (1983).

[11] M. Ambrosio et al., Phys. Lett. 115B, 495 (1982).

[12] R. Battiston et al., Phys. Lett. 127B, 472 (1983).

[13] A. Breakstone et al., preprint CERN-EP-84-105, 1984.

[14] N. Amos et al., Phys. Rev. Lett. 61, 525 (1988).

[15] R. E. Breedon et al., Phys. Lett. 216B, 459 (1989).

[16] N. Amos et al., Phys. Lett. 247B, 127 (1990).

[17] N. Amos et al., preprint FERMILAB-PUB-91-267, 1991.

[18] N. Amos et al., Nucl. Phys. B262, 689 (1985).

[19] C. Augier et al., Phys. Lett. 316B, 448 (1993).

[20] N. Amos et al., Phys. Rev. Lett. 63, 2784 (1989).

[21] F. Abe et al., preprint FERMILAB-PUB-93-232-E, 1993.

[22] J. Whitmore et al., Phys. Lett. 59B, 299 (1975).

[23] N.A. Amos et al., (E710) Phys. Lett. B243, 158 (1990); N.A. Amos et al., (E710) Phys. Lett. B301, 313 (1993).

[24] B.E. Ansorge et al., Z. Phys. C33, 175 (1986).

[25] D. Bernard et al., (UA4) Phys. Lett. B186, 227 (1987).

[26] G.J. Alner et al., (UA5) Phys. Rep. 154, 247 (1987).

[27] J.C.M. Armitage et al., Nucl. Phys. B194, 365 (1982).

[28] M.G. Albrow et al., Nucl. Phys. B108, 1 (1976).

[29] J. Schamberger et al., Phys. Rev. Lett. 34, 1121 (1975).

[30] A.A. Arkhipov. Proceedings of the workshop on soft physics, eds. G. Bugrij, L. Jenkovsky, E. Martynov. Kiev - 1994, p.120.
Strong Interactions at Long Distances, ed. L.L. Jenkovsky. Hadronic Press, Palm Harbor, FL U.S.A., p. 73–79, 1995.

[31] A.A. Arkhipov, P.M. Nadolsky, preprint IHEP 97-6, Protvino 1997.

[32] N.N. Bogoljubov, A.A. Logunov, I.T. Todorov, A.I. Oksak. General Principles of Quantum Field Theory. Moscow, "Nauka", 1987.

[33] A.A. Arkhipov. Sov. J. Theor. Math. Phys. V.83, 247 (1990).

[34] M. Froissart. Phys. Rev. V.123, 1053 (1961).

[35] A.A. Arkhipov, V.I. Savrin. Sov.J. Theor. Math. Phys. V.16, 328 (1973); V.19, 320 (1974).

[36] A.A. Arkhipov, V.I. Savrin. Sov.J. Theor. Math. Phys. V.24, 78 (1975).

[37] A.A. Arkhipov. Sov.J. Theor. Math. Phys. V.49, 320 (1981).

[38] A.A. Arkhipov, V.I. Savrin. Sov.J. Theor. Math. Phys. V.49, 3 (1981).

[39] A.A. Arkhipov. Rep. on Math. Phys. V.20, 303 (1984).

$\sqrt{s}$ (GeV)	σ_{tot} (mb)	$\delta\sigma_{stat}$ (mb)	$\delta\sigma_{sys}$ (mb)	$\sigma_{tot}/2\pi$ (GeV^{-2})
9.78	43.10 ± 0.94	0.80	0.50	17.62 ± 0.39
11.54	43.05 ± 0.12	0.06	0.10	17.60 ± 0.05
13.76	42.12 ± 0.13	0.08	0.10	17.22 ± 0.05
13.86	42.33 ± 0.14	0.14	0.00	17.30 ± 0.06
15.06	41.70 ± 0.18	0.15	0.10	17.04 ± 0.07
16.83	41.79 ± 0.20	0.17	0.10	17.08 ± 0.08
17.91	41.69 ± 0.18	0.15	0.10	17.04 ± 0.07
19.42	41.51 ± 0.15	0.15	0.00	16.97 ± 0.06
19.42	41.44 ± 0.21	0.18	0.10	16.94 ± 0.08
21.26	41.90 ± 0.20	0.20	0.00	17.13 ± 0.08
22.96	41.91 ± 0.21	0.21	0.00	17.13 ± 0.09
30.40	42.13 ± 0.64	0.57	0.30	17.22 ± 0.26
30.63	42.80 ± 0.35	0.35	0.00	17.49 ± 0.14
52.59	43.32 ± 0.35	0.34	0.10	17.71 ± 0.15
52.82	44.71 ± 0.46	0.46	0.00	18.28 ± 0.19
62.29	44.12 ± 0.44	0.39	0.20	18.03 ± 0.18
62.71	45.14 ± 0.38	0.38	0.00	18.45 ± 0.16
540	66.80 ± 7.13	5.90	4.00	27.30 ± 2.91
540	66.00 ± 8.60	7.00	5.00	26.98 ± 3.52
546	61.26 ± 0.93	0.93	0.00	25.04 ± 0.38
546	61.90 ± 1.50	1.50	0.00	25.30 ± 0.61
899	65.30 ± 2.40	0.70	2.30	26.69 ± 0.98
1800	80.03 ± 2.24	2.24	0.00	32.71 ± 0.92
1800	72.80 ± 3.10	3.10	0.00	29.76 ± 1.28

Table I. The $p\bar{p}$ total cross-sections
(statistical and systematic errors added in quadrature).

$\sqrt{s}$ (GeV)	lnA	B (GeV^{-2})	$\chi^2/d.o.f.$
9.78	4.552 ± 0.016	11.66 ± 0.13	0.86
11.54	4.428 ± 0.011	11.67 ± 0.10	0.41
13.76	4.493 ± 0.037	11.47 ± 0.24	0.54
16.26	4.346 ± 0.052	10.74 ± 0.35	0.86
18.17	4.30 ± 0.042	11.06 ± 0.24	0.88

Table II. Fitted parameters.
$d\sigma/dt = Aexp(Bt)(mb/GeV^2)$
$(0.0375 \leq -t \leq 0.4(GeV^2))$

$\sqrt{s}$ (GeV)	B (GeV^{-2})	References
9.78	11.66 ± 0.13	[5]
11.54	11.67 ± 0.10	[5]
11.54	11.6 ± 0.2	[5]
13.76	11.47 ± 0.24	[5]
13.76	11.4 ± 0.6	[22]
13.76	13.2 ± 1.2	[7]
16.26	10.74 ± 0.35	[5]
18.17	11.06 ± 0.24	[5]
19.42	17.0 ± 3.6	[7]
24.3	12.3 ± 0.5	[15]
24.3	12.51 ± 0.11	[15]
30.5	11.37 ± 0.60	[13]
52.6	13.03 ± 0.52	[18]
52.8	13.36 ± 0.53	[9]
52.8	13.6 ± 2.2	[6]
52.8	13.92 ± 0.43	[11]
62.3	13.47 ± 0.52	[18]
540	17.1 ± 1.0	[10]
540	17.2 ± 1.0	[8]
540	17.6 ± 1.0	[12]
541	15.52 ± 0.07	[19]
546	15.28 ± 0.59	[21]
546	15.3 ± 0.3	[12]
546	15.35 ± 0.19	[21]
1800	16.3 ± 0.3	[16]
1800	16.3 ± 0.5	[20]
1800	16.98 ± 0.25	[21]
1800	16.99 ± 0.47	[17]
1800	17.2 ± 1.3	[14]

Table III. Data on the slope at $t \simeq 0$ in $p\bar{p}$ scattering
(statistical and systematic errors added in quadrature).

$\sqrt{s}$ (GeV)	$\sigma_{SD}^{pp}(mb)$	References
20	4.9 ± 0.55	[1]
200	4.8 ± 0.9	[24]
546	5.4 ± 1.1	[26]
546	7.89 ± 0.33	[1]
546	9.4 ± 0.7	[25]
900	7.8 ± 1.2	[24]
1800	9.46 ± 0.44	[1]
1800	11.7 ± 2.3	[23]
1800	8.1 ± 1.7	[23]

Table IV. Data on $p\bar{p}$ single diffraction cross sections.

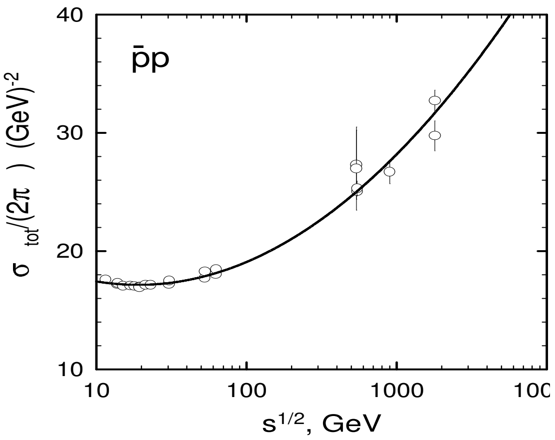

Fig. 3

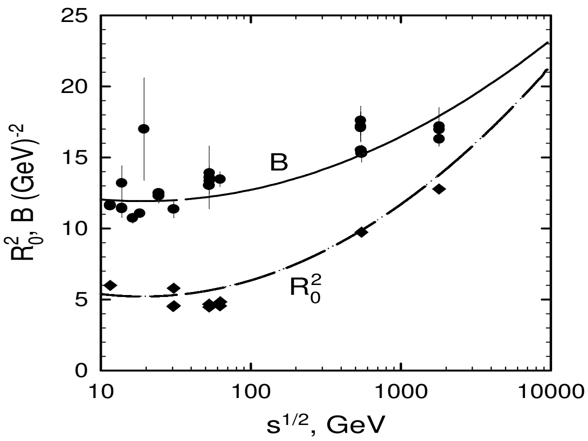

Fig. 4

Fig.5

Fig. 6